

Design and Analysis of a Remotely Operated Mini Forklift Bot

S Mohapatra ^{1*}, A Kumar ², J Rautaray ³

¹Assistant Professor, Department. of Mechanical Engineering., Gandhi Institute for Education and Technology, Baniatangi, Bhubaneswar, India

^{2,3}Student, Department. of Mechanical Engineering., Gandhi Institute for Education and Technology, Baniatangi, Bhubaneswar, India

Abstract. This work is concerned with the design, analysis and programming of a scaled down version of an electric forklift robot. An advantageous consequence of this device is the development of space saving storage units that allow for efficient packing of lighter goods into areas that while not built for human movement, allow ample space for movement of our forklift bot. This is especially important in cases where each cubic meter of the storage unit is valuable, for example, refrigerated goods storage units. Each part of the robot was either carefully selected or designed from scratch in the pursuit of maximizing the load bearing capacity to design-weight ratio. As such, structural analysis was conducted for each part using the Ansys Workbench simulation package. Furthermore, motors that were operated using standard electronic circuits were installed to remotely control the traversal of the bot, while cameras and sensors were employed to monitor its surroundings and movements. The next step was to program the logic circuit and link the various components wired to it. Here the main control device used was an Arduino, which is an integrated open-source electronic platform that allows for precision control of the various electronic components in accordance with the operator's inputs. The hardware used for passing instructions to the Arduino was a common smart phone on which a self-developed android app was installed. Writing a program for this involves careful calibration of the power and position of the driving components and the electric signals they receive.

1 Introduction

The main aim of this undertaking was to provide a possible storage solution for light weight goods by utilizing the technological advantages of robots and robotic circuits to create a Remotely Controlled Forklift Bot. The key motivation for implementing this idea is the development of space saving storage units that allow efficient packing of lighter goods into areas that are not built for human movement but are spacious enough for robots. This is especially important in cases where each cubic meter of the storage unit is essential and costly, for example refrigerated goods storage. While this is an extreme case of automation, the Forklift Bot can also be utilized as an assistant/aid to existing personnel in order to build a hybrid loading and unloading workforce. This synergy between man and machine is the most optimum form of efficient labor.

The forklift prototype is a four-wheeled robot that has the ability to follow directions provided by the operator. There are four wheels including two driving

wheels controlled by two motors and two free wheels in front that are able to rotate by 165°.

This bot is designed to be controlled by a powerful and versatile circuit called an 'Arduino' which is an integrated open-source electronics platform that allows for precision control of the various electronic components in accordance with the operator inputs. The hardware used for passing instructions to the Arduino is a common smart phone on which a self-developed android app can be installed. Signals are wirelessly transmitted from the phone to the Bluetooth module on board the logic unit. Writing a program for this circuit involves careful calibration of the power and position of the driving components to the electric signals they receive.

The design was carried out in four stages which are listed below:

- a) theoretical design and analysis,
- b) material selection and part fabrication,
- c) electronic hardware selection and testing
- d) programming the Arduino and the android app.

* Corresponding author: hemaautorobo@gmail.com

Initial designs and modelling were conducted on 'SpaceClaim' which is a modelling software bundled with the ANSYS package. All dimensions and specifications were decided based on the available components in the market or to accommodate these standard parts. Mechanical equations and laws and subsequent calculations based on them were responsible for determining many of the dimensions and specifications.

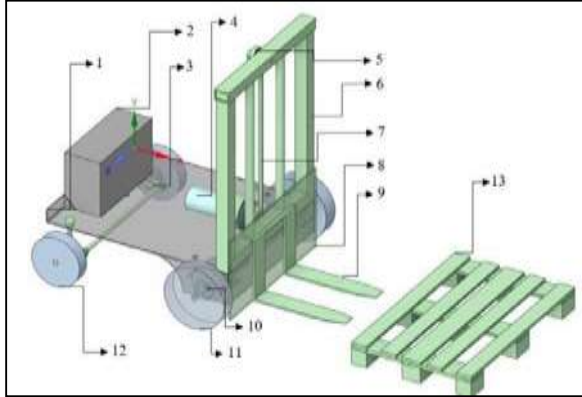


Fig. 1. Final Assembly labeled as follows:

- | | | |
|------------------|---------------------|-------------------|
| 1- Body/Base | 5- Top Pulley | 9- Forks/Tynes |
| 2- Battery | 6- Aluminum Frame | 10- Driving Motor |
| 3- Rear Axle | 7- GT-2 Timing Belt | 11- Front wheels |
| 4- Lifting Motor | 8- Plywood Backrest | 12- Rear Wheels |
| | | 13- Pallet |

2 Part design

The various materials and parts required for this project were selected from local vendors and supply chains. The structural components were manufactured from base materials like sheet metal, aluminum channels, etc. Some components had to be ordered via sellers based on the internet. The delivery times, overseas or local, and the costs had to be balanced in order to get the part in time as well as minimize the cost.

Body

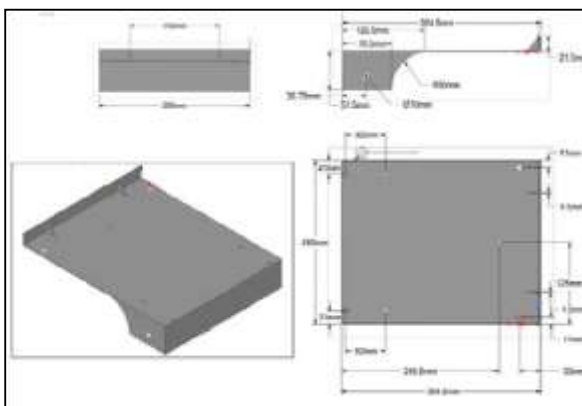


Fig. 2. Front, side, top and isometric view of body.

Figure 2. shows the basic shape of the Part: Body, along with the position and sizes of the various holes required for bolts and joints. The front of the Body is boxed out since it is the load carrying area while the back has an upraised strip supported by triangular pieces which also function to carry the battery (counter weight). The 10 mm holes shown in the side view are provided for the main driving motor axle while the two 8 mm holes on the back are made for the rear wheel supports. The surface of the base is lined with multiple holes of varying sizes for fixing the lift component, drive components and the electronic components. Material used was SS 304 cold rolled Sheet metal 1.5 mm thick.

Drive Components

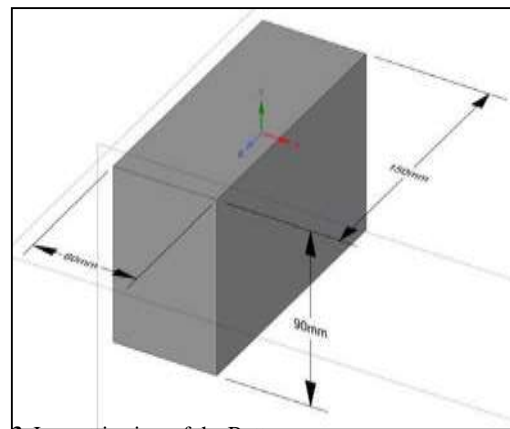


Fig. 3. Isometric view of the Battery.

Figure 3 shows a lead acid type battery with the following specifications:

- Input Voltage: 12 V;
- Output Voltage: 12 V;
- Output Power Wattage: 86.4 Watts;
- Mass: 2.2 kg.

Figure 4 shows one of the heavy duty silicon Wheels of 100mm diameter. Silicon Rubber has a particularly high coefficient of friction and is highly durable. The wheel body is made of ABS + 20% glass fiber for additional reinforcement.

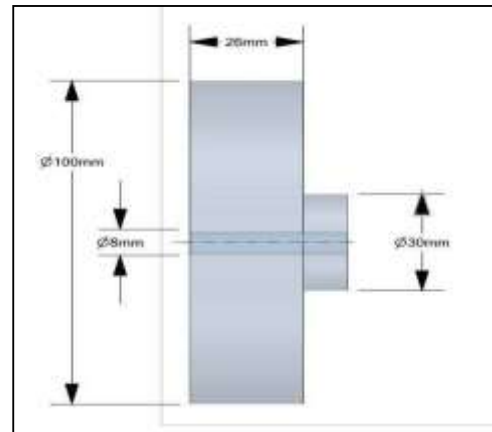


Fig. 4. Front view of wheel.

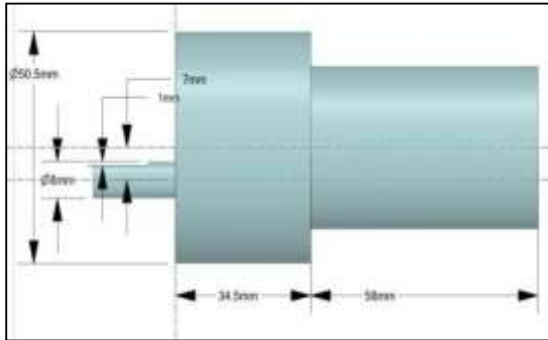


Fig. 5. Front view of motor.

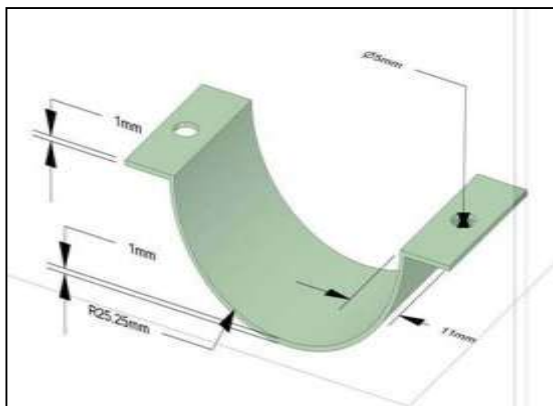


Fig. 6. Isometric view of motor clamp.

The motor was selected primarily based on two parameters, the motor speed and torque. The tractive torque required to move the bot from rest is compared with the Full Load torque (T_f) in Kg-cm times two since there are two motors.ie.

$$40 \times 2 = 80 \text{ Kg} - \text{cm.} \quad (1)$$

We take a factor of safety of 2 since we would like to avoid fully loading the motor.ie.

$$T = T_f / 2 = 40 \text{ kg} - \text{cm} \quad (2)$$

The wheel radius (R) is 5 cm.

The entire robot assembly + load comes to be less than 8 kg (normal force N), then the required tractive torque (T_t) to move the bot in static condition is given by

$$T_t = \mu \cdot N \cdot R = 0.8 \cdot 8 \cdot 5 = 32 \text{ Kg} - \text{cm} \quad (3)$$

Where, μ is the maximum coefficient of friction between SILICON rubber and flooring.

Therefore, since $T > T_t$, the motor is capable of moving the bot at maximum load.ie. static friction. As the bot starts moving rolling friction comes into play which is significantly smaller.

In figure 5, the RS-50 Geared motor with the specified dimensions is shown. The motor specifications are as follows:

Table 1. RS-50 Geared motor specifications

Operating Voltage Range	6 V to 15 V DC
Recommended Voltage (DC)	12 V
Rated RPM (at 12V)	100
Rated Torque (Kg-cm)	8
Full (Stall) Load Torque (Kg-cm)	40
No-load Current (A)	0.2
Full Load Current (A)	1.2
Base Motor Dimensions (mm)	35.5 x 58 (D x L)
Gear box Dimensions	50.5 x 34.5 (D x L)
Motor Shaft Length (mm)	21
Shaft Diameter (mm)	8
Motor Shaft Type	D
Weight (gm)	292

$$W \times H \times D = 15 \text{ cm} \times 9 \text{ cm} \times 6 \text{ cm};$$

Figure 6. shows the general shape of a mild steel motor clamp used to fix the motor to the base.

Lift Assembly

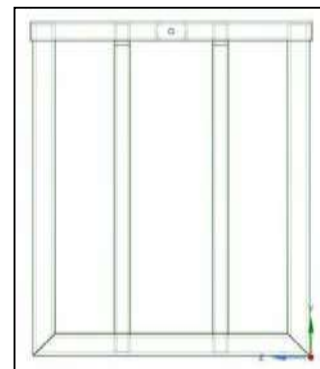


Fig. 7. Lift Frame Assembly.

Figure 7 shows the geometric model of the assembled lift frame. The base channel is angle ground on its ends at 45 degrees to make angled joints with the two side channels using internal brackets and screws. It is a technique commonly used for making aluminum window frames. It also has two circular holes cut into its upper lateral face in order to accommodate the sliding rods. The side channels are not angled at the top so that the

cap is able to slide onto them and be fastened with the slider rods.

The topmost part, named the cap is a channel that is just a few mm larger than the other three and has holes cut out on one of its lateral sides; these holes correspond to the two left and right channels and the two slide rods.

The material chosen for this particular application was **Aluminum 6061** in a square tube form.

Figure 9; the top of the L shaped Tyne has a curved slider plate. The holes in this plate are of the same size as the OD. Of the slider rods which allow free vertical sliding movement. The Material used was Stainless Steel 304L. The sliding plate is attached to a GT2 timing belt using a belt clamp and bolts. The lifting motor can then raise or lower the forks via tension in the timing belt.

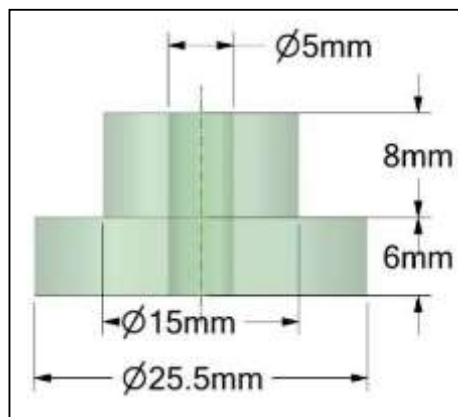


Fig. 8. Lift Pulley.

Figure 9 shows the load carrying member of the Lift assembly. Also known as the tynes, these make direct contact with a load that is to be transported. These are attached to the forklift carriage and are designed to carry a load from the bottom. The tip of the fork is thinned out since the majority of stress is experienced at the base of the cantilever (fork). The tip is also tapered when seen from the top view, this is to allow sliding of pallet base into position in case of mismatch or improper position of the forklift.

Figure 10 shows timing belt having 6mm width and 310 mm length loop. i.e. $\text{circumference of pulley} + 2 * \text{lift height}$. Figure 11 is a Lift Pulley 6mm width. This pulley drives the belt and is mounted onto the motor which is clamped at the base of the Frame. Another pulley is mounted at the top (cap) center.

Wooden Load Backrest was made from 3 mm plywood and backrest provides the operator another surface to rest the load against and is attached to the Tynes. This helps prevent the load from slipping backwards during lifting and travel conditions. The

forklift backrest provides stability when carrying loads of irregular dimensions.

The motor is rated to produce 40 Kg-cm torque after taking factor of safety 2. Tension in the belt is equal to the weight of the Load being lifted. This tension is generated by the teeth of the pulley. The maximum force the can be applied at the tip of the pulley ;

$$F_p = 40/12.75 = 3.137 \text{ Kg} = 30.77 \text{ N} \quad (1)$$

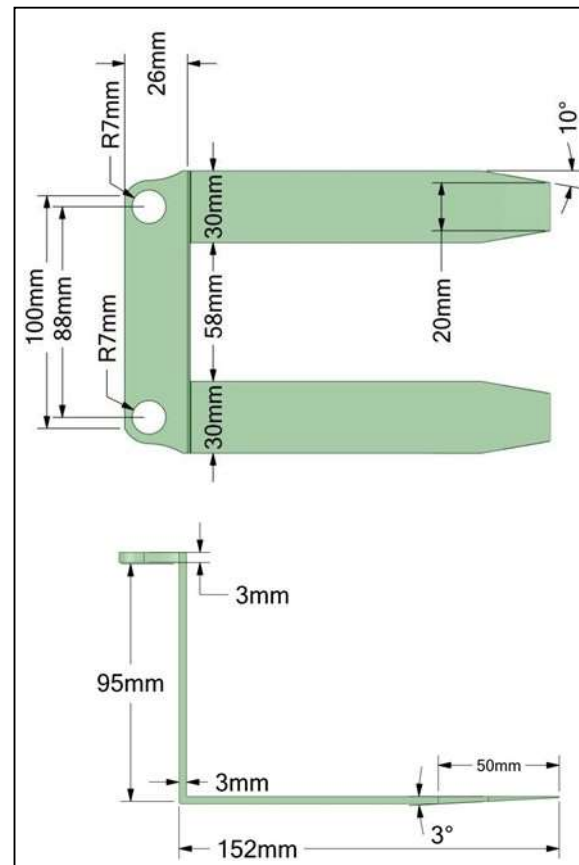


Fig. 9. Fork/Tynes front and top view.

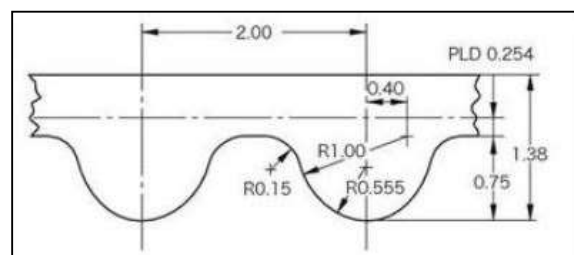


Fig. 10. Timing belt Section; dimensions in mm.

The neoprene and fiberglass belt in fig. 10, is rated to be able to withstand working tensions of above 100 N. Hence, the safe load carrying capacity of the lift is approx. 3 kg or 30 N. A belt clamp is employed to fix it to the forks.

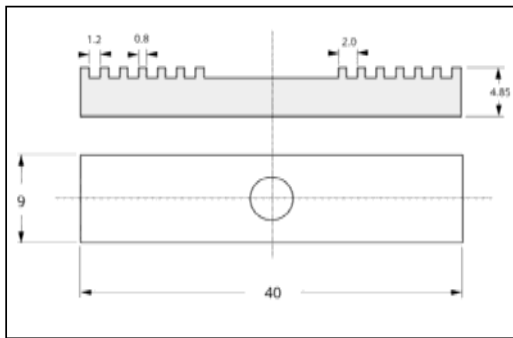


Fig. 11. GT-2 timing belt clamp; dimensions in mm.

Steering mechanism

Figure 12 illustrates the Steering Rod, used to transmit the steering force to both wheel axles. Figure 13 is Steering Axle and is coupled to the wheel and transmits steering torque to turn the rear wheels. It has two projections that have concentric holes of equal diameters drilled through them which align with the hole present at the ends of the steering rod. Any lateral movement in the rod causes a steering torque to be produced at the axle.

Steering Force required:

$$F_s = \mu * m * g * F_s = \mu * m_c * g \quad (1)$$

Where μ is the coefficient of friction between the rear wheel and floor, m_c is the Corner Mass acting on one rear wheel, g is the acceleration due to gravity.

Steering torque required at joint:

$$T_s = F_s * R \quad (2)$$

Maximum torque that can be produced by servo at joint:

$$T_m = T_R * R/r \quad (3)$$

Where T_R is the rated torque of servo motor; R is the distance between axis of joint and the axis of rotation of the steering block; r is the radius of the servo motor arm attached to its axle.

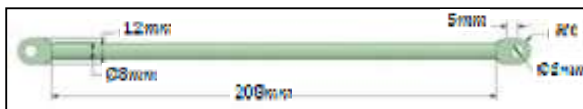


Fig. 12. Steering Rod.

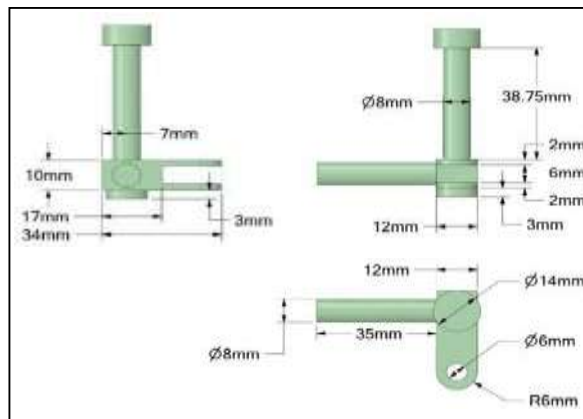


Fig. 13. Steering Block/Axle.

Figure 14, illustrates the steering assembly at three different angles of rotation. The horizontal component of displacement between the fixed joint and the rotating pivot is provided by the servo motor connected to the steering rod. Thus, the servo motor controller is calibrated with the Arduino to precisely rotate the wheels at any angle between the two limits.

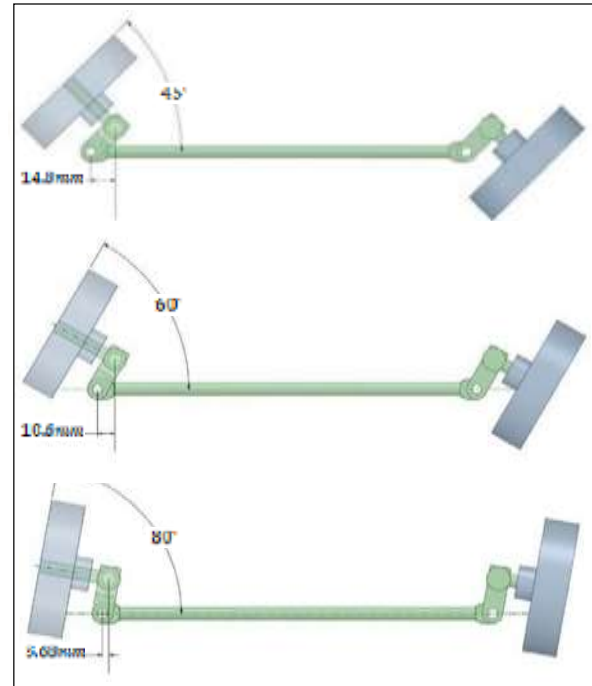


Fig. 14. Steering assembly at different degrees of rotation.

3 Part list

Every part that was either selected or manufactured is listed below along with their respective costs in INR:

Since two forks are used to lift the load:

$$MBS = 49.7/2 \frac{N}{mm^2} = 24.85 \frac{N}{mm^2} \quad (6)$$

Fork as cantilever; shear stress:

In contrast to bending moment, the maximum shear stress is developed at the centroidal axis. i.e. $y = 0$.

Shear Stress at centroidal axis is given by:

$$\text{Shear stress} = \frac{VQ}{Ib} \quad (1)$$

Here, V is the shear force acting at base cross section;

Q is the first moment of inertia of the upper half;

I is centroidal moment of inertia;

b is the breadth of the cross section.

$$V = 3 \times 9.81 \quad (2)$$

$$Q_{\text{maximum}} = \frac{bh^2}{8} \quad (3)$$

$$I = 67.5 \text{ mm}^4 \quad (4)$$

$$\text{Maximum Shear Stress} = 0.218 \frac{N}{mm^2} \quad (5)$$

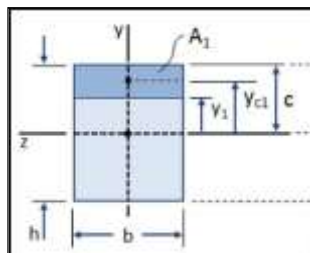


Fig. 16. Fork as a beam, cross-section.

5 Static analyses

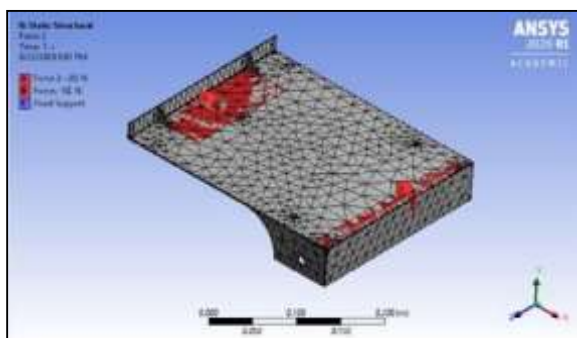


Fig. 17. Body: Setup.

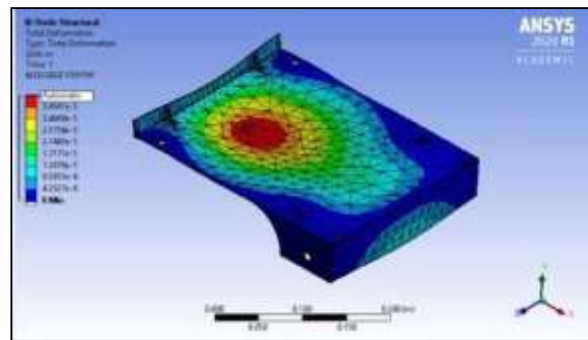


Fig. 18. Body: Total Deformation map.

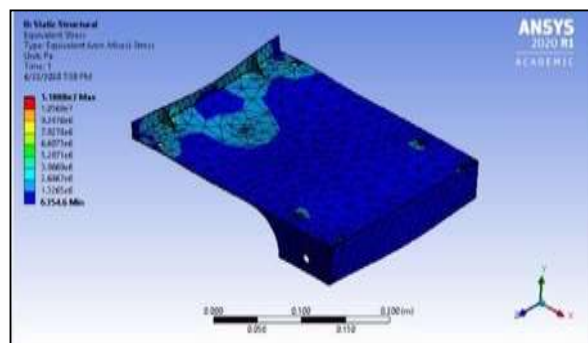


Fig. 19. Body: Equivalent Strain map.

From the above conducted analyses on the forklift body we observe the following:

- Fig. 18, the maximum displacement is found to be just in front of where the battery is to be placed. It is well under acceptable levels of displacement for the body material but for additional safety, a single strip of steel can be run laterally to counteract any unpredictable sharp increase in deflection.
- Fig. 19, the maximum equivalent stress is well below the allowable stress for the body material.

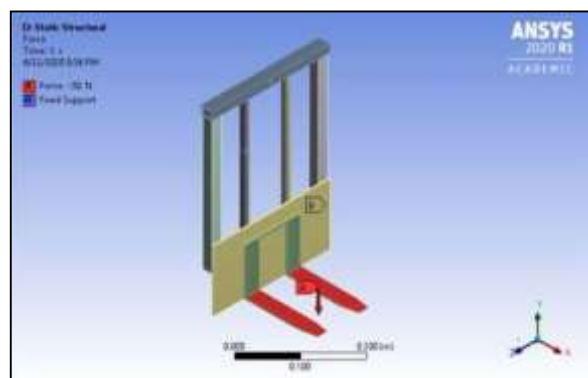


Fig. 20. Lift Assembly: Setup.

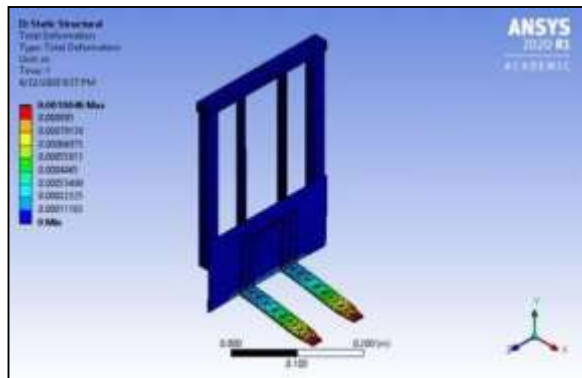


Fig. 21. Lift Assembly: Total Deformation map.

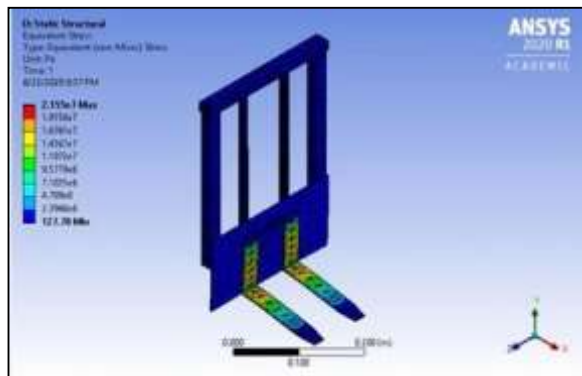


Fig. 22. Lift Assembly: Equivalent Stress map.

From the above conducted analyses on the Lift assembly we observe the following:

- Fig. 21, the maximum displacement occurs at the tip of the forks and is less than the theoretical allowable displacement levels.
- Fig. 22, the maximum equivalent stress is greatest at the base of the forks and is below the allowable stress values of the selected material.

6 Operation procedure

For this particular type of bot, a front wheel drive was preferred over a rear wheel drive simply because of the increased maneuverability during loading and unloading; particularly in reverse motion.

The Arduino program to control each motor was written in C++. A Bluetooth module connected to the Arduino functions as a signal receiver. These control signals are also emitted by the Bluetooth module inside a regular smartphone running a custom-made android application.

After installing and opening the .apk file, two translucent virtual joystick UI elements offset from the center on either side, placed on top of a full screen camera feed, are visible. This live video stream is captured by the camera fixed to the front of the forklift.

Sliding the left joystick north will accelerate the bot forward whereas sliding it to the south reverses its motion. The servo motor responsible for operating the steering mechanism is controlled by the east-west movement of this joystick.

The right joystick controls the vertical movement of the Tynes which are a part of the lift mechanism.

The centers of the joysticks signal zero voltage while the extremities signal maximum voltage supply. There is a linear gradient of velocity values in the region between the center and the extremities.

Steps for routine operation

Standard operation for lifting a loaded palette then placing it is as follows:

1. Use the left joystick to coordinate hand to eye movement while watching the camera feed.
2. Line both forks that are visible at the bottom of the video with the slots beneath the palette.
3. Drive forward until forks are completely hidden by the palette.
4. Use the left joystick to slightly lift the load off the ground.
5. Move to the storage location.
6. Depending on whether the load is to be placed on the upper level or on the ground, operate the lift accordingly making sure to securely place the palette down.
7. Drive the forklift in purely reverse motion until the forks are fully removed from under the palette.
8. Operate the lift to its zero position, i.e. the ground level.

Precautions

1. Make sure that the forks are at zero level before driving the bot.
2. Check that the weight of the load is equal to or below the load rating of the forklift bot.
3. Slow down during turns.
4. Do not abruptly leave the joystick especially when carrying loads in order to prevent sudden motor braking.
5. If smoke is observed from any electrical component, immediately stop operation and disconnect the battery.

7 Results and conclusions

Design and Selection of Components

The various parts and components were designed and selected based on calculations.

The driving motors needed to produce 32 kg-cm of maximum force in order to start the bot from rest against static friction. We selected motors with 40 kg-cm rating at half load.

The lifting motor could produce a force of 30.77 N at the tip of our pulleys, i.e. a maximum load of 30 N or roughly 3 kg was decided as the lifting capacity of the forklift.

The total mass of the Forklift was determined to be around 4.8 kg by assigning the appropriate materials from the ANSYS material library and conducting volume and mass calculations within the program. This mass was compared to the lifting capacity of the bot.

It was found that the ratio of maximum load capacity to the mass of the forklift is 5:8 or 1:1.6, which is a preferred weight ratio.

The tynes were assumed to be cantilever beams with rectangular cross sections bearing a uniformly distributed load over its entire surface of 3 kg. This allowed us to calculate the approximate maximum bending stress of ~25 MPa, and maximum Shear Stress of 0.21 MPa.

Balancing calculations in static conditions gave an anti-clockwise moment of 1548 N-mm at the front wheels which was balanced by the rear wheel reaction forces produced by the roller supports.

Modelling and Assembly

The design model was realized in the SpaceClaim modelling environment and the final assembly was produced. Each part was checked for dimensional inaccuracies and fillets were applied to sharp edges.

Finally, all the models had to undergo face splitting in order to generate the exact faces on which loads and supports can be applied.

Static Structural Analysis

Load bearing members were subjected to static structural analysis to confirm the design decisions and to find any stress concentrated areas. This was done by first establishing connections and joints and then applying boundary conditions i.e. supports and displacements at the appropriate areas and subjecting them to loading conditions.

The analysis of part named;

Body resulted in acceptable maximum displacement, 0.03mm, maximum stress, $5.28 \times 10^6 \text{ Pa}$, and maximum strain, 2.72×10^{-5} , values.

The analysis of part named;

Tynes resulted in acceptable maximum displacement, 1mm at the fork tips, maximum stress, $2.1 \times 10^7 \text{ Pa}$, and maximum strain, 1.69×10^{-4} , values.

We can see that the values obtained from the analysis data in case of maximum stress at the base of the forks of 21MPa is close to the value calculated by approximating it to a cantilever beam and calculating the maximum bending stress of 25 Mpa. The difference obtained is believed to be due to the partial sharing of load at the top bend of the tynes and the wooden backrest.

The various parts and components were designed and selected based on theoretical calculations which were tallied with the experimental results obtained from the analysis software.

The driving motors needed to produce 32 kg-cm of maximum force in order to start the bot from rest against

static friction. We selected motors with 40 kg-cm rating at half load.

The lifting motor could produce a force of 30.77 N at the tip of pulleys and a maximum load of 30 N or roughly 3kg was decided as the lifting capacity of the forklift.

The total mass of the Forklift was determined to be around 4.8 kg by assigning the appropriate materials from the Ansys material library and conducting volume and mass calculations within the program. This mass was compared to the lifting capacity of the bot.

It was found that the ratio of maximum load capacity to the mass of the forklift is 5:8 or 1:1.6, which is a preferred weight ratio.

The tynes were assumed to be cantilever beams with rectangular cross sections bearing a uniformly distributed load over its entire surface of 3kg. This allowed us to calculate the approximate maximum bending stress as ~25 MPa and maximum Shear Stress as 0.21 MPa.

Balancing calculations in static conditions gave an anti-clockwise moment of 1548 N-mm at the front wheels which was balanced by the rear wheel reaction forces.

References

1. Burinskiene: "The Travelling of Forklift in Warehouse". Retrieved 2008-01-22.
2. Saurabh S Shah, Mohd Husain A Sunasara, Pramit S Jain, Zohaib Shirgaonkar, Department of Mechanical Engineering, Prof. Jugal Jagtap," (IJERT) ISSN: 2278-0181, **9(6)**, (2020).
3. Burinskiene. December 2011, IJSM10(4), Int j simul model **10** (2011)
4. Rajat.Rajendra. Wade, Digvijay. K. Take, Mahesh. S. Deshmukh, Pranaw. A. Raut, (IRJET), **05** (2018)
5. Kaushik S. Panara, Vivek R. Mishra, Amrat M. Patel, Amrat M. Patel, Tushar B. Patel, Krunal R. Dhivar IJSTE – **2(4)** (2015)
6. Anil A. Sequeira1, Saif Mohammed, Avinash A. Kumar, Muhammed Sameer, Yousef A. Kareem, Krishnamurthy H. Sachidananda, IJIETA (2019)
7. Dr. Pravin Potdukhe, IJRAT, **7(4)**, (2019)
8. P. Naveenkumar, N. Ashok, J. Dinesh Kumar, S. Mohamednizarudeen, (IJERT) **6(4)**, (2018).